

# Fragility Assessment of Light-Frame Wood Construction Subjected to Wind and Earthquake Hazards

Bruce R. Ellingwood, M.ASCE<sup>1</sup>; David V. Rosowsky, M.ASCE<sup>2</sup>; Yue Li, S.M.ASCE<sup>3</sup>; and Jun Hee Kim<sup>4</sup>

**Abstract:** A fragility analysis methodology is developed for assessing the response of light-frame wood construction exposed to stipulated extreme windstorms and earthquakes. Performance goals and limit states (structural and nonstructural) are identified from a review of the performance of residential construction during recent hurricanes and earthquakes in the United States. Advanced numerical modeling tools provide a computational platform for risk analysis of light-frame wood building structural systems. The analysis is demonstrated for selected common building configurations and construction (defined, e.g., by roof sheathing, truss spacing, and roof or shear wall nailing patterns). Limit state probabilities of structural systems for the performance levels identified above are developed as a function of 3-s gust wind speed (hurricanes) and spectral acceleration (earthquakes), leading to a relation between limit state probabilities and the hazard stipulated in ASCE Standard 7, "Minimum design loads for buildings and other structures."

**DOI:** 10.1061/(ASCE)0733-9445(2004)130:12(1921)

**CE Database subject headings:** Building codes; Earthquakes; Hurricanes; Probability; Timber construction; Wooden structures; Framed structures.

## Introduction

Housing represents an enormous social investment in the United States (for most individuals, it is their largest single asset). The majority of residential buildings in the United States (approximately 90%) are light-frame wood construction. The primary framing material in residential construction is dimension lumber, which is often used in combination with other wood products such as plywood, I-beams, oriented strand board (OSB), and laminated veneer lumber National Association of Home Builders (NAHB 1999a,b).

Residential buildings with light-frame wood construction are especially susceptible to extreme winds. Four recent hurricanes—Hugo, Andrew, Opal, and Iniki—have caused tremendous damage to residences in coastal regions. Hurricane Hugo (1989) caused insurers to pay out \$6.0 billion most of which was residential damage claims. (All insured losses are given in 2001 \$U.S., with the exception of losses due to Hurricanes Opal and Iniki, which are given in 1997 \$U.S. ([www.giis.org/disaster.html](http://www.giis.org/disaster.html).) Hurricane Andrew (1992) produced insured property losses estimated at

\$20.2 billion; catastrophic failures of one- and two-story light-frame residential buildings were the most frequently observed mode of building damage. In the same year (1992), Hurricane Iniki caused \$1.8 billion in damage. Damage during Opal (1995) was close to \$ 2.2 billion. Population growth in hurricane-prone areas is increasing, raising the prospects of even higher damages and losses in the future. Losses to residential construction during recent earthquakes (Loma Prieta, Northridge) have been similarly severe. The majority of fatalities in the Northridge earthquake (24 out of 25), and more than half of the estimated \$16.7 billion insured loss was due to damage to wood buildings (Schierle 2001).

In summary, damage to residential building construction incurred due to extreme hurricane winds and earthquakes during the past 15 years has led to insured losses in excess of \$U.S. 45 billion and total losses that are far in excess of this value. The aftermath of these natural disasters has led to intense professional and public scrutiny of real or perceived deficiencies in design and construction practices, building codes, and their enforcement. This scrutiny has pointed to the need for an improved basis for designing new residential construction and for assessing the condition of the current residential building inventory and its vulnerability to future hazards. Such improvements to building practices require tools for evaluating new and existing building products, for modeling the uncertainties that are inherent to the prediction of building performance, and for managing the risk that is consequent to these uncertainties economically.

Protection of building occupants against injury or loss of life is of paramount importance in structural design. Thus the main objective of current codes and standards is to prevent building failures leading to loss of life during rare events. While this objective has been essentially achieved for buildings in the United States subjected to windstorms or earthquakes, the economic losses and social disruption associated with many of these events have become unacceptable. It has become apparent that buildings designed by code, which satisfy the life safety objective, may not meet other expectations of building owners and occupants.

<sup>1</sup>College of Engineering Distinguished Professor, School of Civil and Environmental Engineering, Georgia Institute of Technology, Atlanta, GA 30332-0355.

<sup>2</sup>Richardson Chair in Wood Engineering and Professor of Civil Engineering, Oregon State Univ., Corvallis, OR 97331-5751.

<sup>3</sup>Graduate Research Assistant, School of Civil and Environmental Engineering, Georgia Institute of Technology, Atlanta, GA 30332-0355.

<sup>4</sup>Graduate Research Assistant, Dept. of Civil, Construction, and Environmental Engineering, Oregon State Univ., Corvallis, OR 97331.

Note. Associate Editor: Daniel Dolan. Discussion open until May 1, 2005. Separate discussions must be submitted for individual papers. To extend the closing date by one month, a written request must be filed with the ASCE Managing Editor. The manuscript for this paper was submitted for review and possible publication on August 29, 2003; approved on March 26, 2004. This paper is part of the *Journal of Structural Engineering*, Vol. 130, No. 12, December 1, 2004. ©ASCE, ISSN 0733-9445/2004/12-1921-1930/\$18.00.

Performance-based engineering (PBE) is a new paradigm that is gaining momentum in the United States. It is motivated by a desire to add value to the building process by ensuring that the building meets the expectations of the building owner, occupants, and the public regarding performance during and following spectrum of events rather than a single “design-basis” event (Hamburger 1996). Performance-based engineering will require more comprehensive and quantitative probability-based procedures for managing risk and uncertainty than are found in first-generation criteria such as LRFD (Ellingwood 1994; Ellingwood 1998; Rosowsky and Ellingwood 2002). To advance building practices for residential construction, this paper presents a general probability-based methodology for assessing the response of light-frame wood construction subjected to specified demands from extreme windstorms and earthquakes.

## Role of Probability in Modern Structural Codes

Modern structural design codes and standards are based on concepts of limit states design (or LRFD, as it commonly is termed), with safety checks that are based on structural reliability theory (Ellingwood 1994). For example, in LRFD of engineered wood structures, the structural safety requirement is expressed by a set of equations (*ASCE standard 16-95*),

$$\lambda\phi R_n > \sum \gamma_i Q_i \quad (1)$$

The design strength on the left-hand side of Eq. (1) is the product of  $R_n$ =nominal resistance of a member, component, or connection adjusted to end use conditions;  $\phi$ =resistance factor that accounts for uncertainty in short-term strength as well as mode of failure; and  $\lambda$ =time-effect factor that takes into account the dependence of wood strength on rate and duration of load. The nominal loads,  $Q_i$ ; and load factors  $\gamma_i$  on the right-hand side of Eq. (1) are defined in Section 2.3 of *ASCE standard 7-02* (2003). The resistance criteria for each limit state in Eq. (1) are based on a reliability-based assessment of and calibration to traditional practice (e.g., Galambos et al. 1982; Ellingwood and Rosowsky 1991).

The LRFD criteria represented by Eq. (1) were calibrated (in a probabilistic sense) to existing practice to facilitate acceptance by structural engineers who design wood structures. This calibration process has raised several issues that must be considered in advancing performance-based design for light-frame wood construction. For one, the calibration was performed only for individual members, components, and connections. System effects were considered only indirectly, through effective length factors in column design, response modification factors used to determine base shear in aseismic design, repetitive member adjustment factors for flexure in joists, truss chords, etc. Accordingly, such checks provide only an approximate indication of how a *system* of such elements might perform during an extreme event.

Furthermore, the reliability benchmarking of structural members that had been properly designed by traditional working stress design codes was essentially a tool for risk communication between reliability specialists working to develop probability-based design, standard-writing groups, and the structural engineering profession. Because of limitations in supporting databases, the reliability benchmarks identified in the calibration process were “notional,” in the sense that no attempt was made to correlate them to structural failure rates observed in service. This failure to reconcile predicted and observed failure rates makes it difficult to

use such methods for forecasting performance of buildings during a natural disaster, for planning and implementing effective post-disaster management strategies, or for setting insurance premium rates. To achieve reasonable agreement (within the limitations imposed by statistical sampling) between calculated and observed failure rates, properly validated system reliability analysis models are essential. This is especially important in light-frame wood construction, where the body of research during the past two decades has indicated that there is an integral relationship between member, connection, and system performance.

Finally, traditional design practice has been focused on the life safety objective, as noted above. There has been little attention paid to serviceability issues, which do not impact life safety but may have a significant social and economic impact. PBE will require a broader view of the purpose of structural design.

## Performance Objectives and Limit States

Performance-based engineering aims at ensuring that a building or other facility achieves the desired performance objectives levels when subjected to a spectrum of natural or man-made hazards. The proposals for PBE that have been published in recent years by organizations such as FEMA, NEHRP, and SEAOC, among others, all have common features. Consistent with current building regulatory practice, they all stipulate that life safety (LS) should be preserved under “severe” events. Beyond this, they stipulate that collapse shall not occur under “extreme” events (collapse prevention, or CP), and that function shall be preserved [continued function or immediate occupancy (IO)] under “moderate” events. (The definitions of what is “severe,” “extreme,” or “moderate” have yet to stabilize, but are likely to be based on the annual probability of exceeding the design hazard or its return period.) As an example, one might require that the building be designed so that there is no disruption of function following an event with 50% probability of being exceeded in 50 years (abbreviated in the sequel as a 50% /50-year event), that life safety is preserved under a 10% /50-year event, and that collapse will not occur under a 2% /50-year event. These general performance objectives are encapsulated in a matrix of performance objectives versus hazard levels. Specific buildings are placed in that matrix by occupancy classification (e.g., Table 1-1 of *ASCE standard 7-02*).

Verification that a building performance requirement is met requires a mapping between the qualitatively stated objective (e.g., immediate occupancy following the 50% /50-year event) and a response quantity and limit state (measuring force or deformation) that can be checked using principles of structural analysis and mechanics. Such a mapping invariably requires that the behavior of the building structural system be considered as a whole. When the performance objective can be related to local damage, a limit state based on member (or connection) strength or deformation may be sufficient. However, the performance of individual members and connections within the system may not be indicative of overall system performance. In light-frame wood construction in particular, a system analysis based on a first-failure limit state may lead to a highly pessimistic view of the capacity of the system to withstand general collapse (Rosowsky and Ellingwood 1991). While it is an oversimplification to equate performance-based design to deformation-based design, deformation of the structural system usually is preferable to member strength when system behavior must be measured through one structural response quantity (normally computed by finite element-based

structural analysis), particularly when the structural response and behavior are in the nonlinear range. There have been a number of recent efforts to relate structural deformations to performance levels. For example, in FEMA Report 356 [and its widely cited predecessor, FEMA Report 273 (1997)] (FEMA 2000), the immediate occupancy, life safety, and collapse prevention performance levels for vertical structural elements in light-frame wood construction subjected to seismic effects are related to transient lateral drifts of 0.01, 0.02, and 0.03, respectively. We will return to this issue in the development of fragilities for wind and seismic effects.

## Structural Risk and Assessment and Fragility Modeling

A probabilistic safety assessment (PSA) provides a structured framework for evaluating uncertainty, performance, and reliability of a building system subjected to wind or earthquake hazards. As a first step in a PSA, one must identify limit states, or conditions in which the structural system ceases to perform its intended functions in some way. Such limit states are expressed in the general form  $G(\mathbf{X}) < 0$ , in which  $\mathbf{X}$  = vector of basic uncertain variables that describe the limit condition, and may be either strength or deformation-related, as noted above. With each of the limit states identified, the probability of a specified limit state can be expressed as

$$P[G(\mathbf{X}) < 0] = \sum_y P[G(\mathbf{X}) < 0 | D=y] P[D=y] \quad (2)$$

in which  $D$  = random variable describing the intensity of the demand on the system (e.g., 3-s gust wind speed; spectral acceleration at the fundamental period of the building, etc.), and  $P[G(\mathbf{X}) < 0 | D=y]$  is the conditional limit state probability, given that  $D=y$ . The term  $P[D=y]$  defines the natural hazard probabilistically. The conditional probability  $P[G(\mathbf{X}) < 0 | D=y] = F_R(y)$  denotes the fragility. The breakdown of risk in Eq. (2) facilitates risk analysis and decision-making. Wind, flood, and earthquake hazards often are determined by governmental agencies such as the National Weather Service or the U.S. Geological Survey. Nowadays, such information often can be retrieved from a website for the particular building site. In contrast, the responsibility for the structural design and, by inference the structural fragility, ultimately lies with the structural engineer.

The fragility is central to the probabilistic safety analysis. It also can be used to assess the capability of a system to withstand a specified demand (say, a 500-year wind or an earthquake with a 10% probability of being exceeded in 50 years; or, even more simply, a magnitude 7 earthquake centered 20 km from the building site). Such safety margins can be useful for engineering decision-making in situations where the hazard curve is technically difficult (or costly) to define. Conversely, the fragility can be used to identify a level of demand at which there is high confidence that the system will survive. The communication of risk to stakeholders in the building process is facilitated and simplified, as the demand (or interface) variable,  $D=y$ , can be selected arbitrarily, depending on the decision at hand.

The fragility of a structural system commonly is modeled by a lognormal cumulative distribution function (CDF). The lognormal CDF is described by

$$F_R(y) = \Phi[\ln(y/m_R)/\zeta_R] \quad (3)$$

in which  $\Phi(\cdot)$  = standard normal probability integral;  $m_R$  = median capacity; and  $\zeta_R$  = logarithmic standard deviation, approximately equal to the coefficient of variation (COV),  $V_R$ , when  $V_R < 0.3$ .

Fragility modeling must be supported by databases to describe the medians and uncertainties in all factors known to affect the ability of the system to withstand challenges from the range of postulated hazards of interest. Sources of uncertainty in the assessment of structural response are reflected in parameter  $\zeta_R$  (or  $V_R$ ). As a natural material, wood structural properties tend to be highly variable (Green and Evans 1987). In addition, wood structural systems are designed and fabricated with a large number of connection and fastener details, most of which are difficult to model mathematically, and construction quality and code enforcement can vary significantly from building to building. Some factors affecting performance of wood structures are inherently random (aleatory) in nature, and thus are irreducible at the current level of engineering analysis. Examples would include strength of wood in tension or in compression parallel-to-grain. Others arise from the assumptions made in the analysis of the system and from limitations in the supporting databases. In contrast to aleatory uncertainties, these knowledge-based (or epistemic) uncertainties depend on the quality of the analysis and supporting databases, and generally can be reduced, at the expense of more comprehensive (and costly) analysis. Sources of epistemic uncertainty in light-frame wood construction include two-dimensional models of three-dimensional buildings, probabilistic models of uncertainty estimated from small data samples, wind exposures of buildings, and similar knowledge-based uncertainties.

## Structural Fragilities for Wind and Earthquake Hazards

Performance limit states for light-frame wood construction exposed to hurricane winds include roof panel uplift due to local wind effects, failure of connections of roof-to-wall leading to uplift of the roof, cracking of interior and exterior finishes, excessive lateral drifts (racking) leading to malfunction of doors and windows, wall-foundation failures, and projectile damage. Insurance claim files from Hurricanes Hugo and Andrew have revealed that the building envelope suffers the most wind damage. Postdisaster surveys of the performance of residential construction during extreme hurricane winds indicate that the roof system is the most vulnerable building subsystem (NAHB 1993). Accordingly, maintaining integrity of the roof system is essential for minimizing economic losses. Roofing and roof panel uplift can lead to severe water damage to the building contents, violating the IO performance objective (e.g., Sparks et al. 1994). In addition, damage or destruction of the roof structural system may cause walls to lose lateral support and lead to building collapse, violating the LS or CP performance objectives (Manning and Nichols 1991). Breaching the building envelope by breaking of windows or doors can be an issue as well, but this failure mode is outside the scope of this paper. For earthquakes, the performance of light-frame buildings is dependent on the integrity of lateral force-resisting systems and their anchorage, and damage can be related to excessive lateral drift of the frame or failure of shear walls that resist lateral forces. In the context of performance-based engineering, these limit states must be mapped to the IO, LS, and CP performance objectives mentioned above (Rosowsky and Ellingwood 2002).

**Table 1.** Wind Load Statistics

Variable	One story without roof overhang		One story with roof overhang		Two story without roof overhang	
	Mean	Standard deviation	Mean	Standard deviation	Mean	Standard deviation
$K_z$ (exposure B)	0.57	0.12	0.57	0.12	0.63	0.12
$K_z$ (exposure C)	0.8	0.12	0.8	0.12	0.84	0.12
$GC_p$ (C & C)	1.81	0.22	3.18	0.38	1.81	0.22
$GC_p$ (MWFRS)	0.86	0.15	0.86	0.15	0.86	0.15
$GC_{pi}$	0.15	0.05	0.15	0.05	0.15	0.05
$K_d$	0.89	0.14	0.89	0.14	0.89	0.14

The strength of wood may be sensitive to the rate and duration of structural load(s) (DOL). However, these DOL effects become pronounced only when the load magnitudes are sustained for an extended period of time (months to years). In the cases considered subsequently in this paper, the duration of the wind or earthquake forces is relatively short (on the order of minutes to hours), and the stresses on the structural elements induced by the other service loads are assumed to be at or below the endurance limit for the material. Accordingly, DOL effects are assumed to be negligible, and are not considered further in this paper.

### Fragility Models for Hurricane Winds

Fragility assessments were performed for light-frame building construction with various roof configurations and construction practices (roof type, slope, roof height, nailing pattern, connector type, and truss spacing) subjected to hurricane winds. These fragilities are conditional, in the sense that failure sequences, initiating from local component failure and developing into partial and complete collapse, are not considered. Such sequences can be developed (e.g., Unanwa et al. 2000), but require a more detailed model of the building system than can be supported by the available test data. Moreover, the survey by Sparks et al. (1994) demonstrated the importance of component failure on insured losses.

Three types of single-family light-frame residential houses were considered as representative of the residential building inventory in the southeast United States: a one-story building with gable roof with roof overhang, a one-story building with gable roof without roof overhang, and a two-story building with gable roof without roof overhang. Roofs on all three building systems had roofs with a 6:12 slope and repetitive roof trusses spaced 24 in. (610 mm) on-center. Roof sheathing was nominally 4 ft  $\times$  8 ft  $\times$   $\frac{1}{2}$  in. (1.2 m  $\times$  2.4 m  $\times$  13 mm) panels. It should be noted that light-frame wood construction traditionally has been non-engineered; thus the roof systems discussed in the sequel represent a mix of prescriptive and experience-based practices, and have not been designed by any specific code requiring either allowable stress or limit states design.

**Table 2.** Dead Load Statistics

Component	Mean	Coefficient of variation	Cumulative distribution function	Source
Roof panel	1.6 psf (0.077 kPa)	0.10	Normal	NAHB (1999a,b)
Roof-to-wall connection	15 psf (0.717 kPa)	0.10	Normal	Rosowsky and Cheng (1999a,b)

Limit states describing roof panel uplift and roof-to-wall connection failures both involve wind load and dead load as counteracting structural actions, expressed as

$$G(R, W, D) = R - (W - D) \quad (4)$$

where  $R$ =resistance of the roof panel to uplift or resistance of the roof-to-wall connection;  $W$ =uplift wind load; and  $D$ =dead load on panel or roof-to-wall connection. Note that dead load counteracts the uplift of the wind, and has a beneficial effect on roof performance.

### Wind Load

The wind pressure acting on low-rise building components and cladding is determined from

$$W = q_h [GC_p - GC_{pi}] \quad (5)$$

in which  $q_h$ =velocity pressure evaluated at mean roof height;  $G$ =gust factor;  $C_p$ =external pressure coefficient; and  $C_{pi}$ =internal pressure coefficient. The velocity pressure is calculated as

$$q_h = 0.00256K_hK_{zt}K_dV^2 \quad (6)$$

in which  $K_h$ =exposure factor;  $K_{zt}$ =topographic factor (taken equal to unity so as not to make the results dependent on local topography surrounding the building);  $K_d$ =directional factor; and  $V$ =3-s wind speed at the height of 10 m (33 ft) in an open-country exposure. [When implemented in *ASCE standard 7*, Eq. (6) includes an importance factor related to building occupancy, the effect of which is to adjust  $V$  to different return periods.] The most severe wind pressures on a roof occur in the regions of flow separation at the eave, ridge, and corners of the roof. Postdisaster surveys of damage from Hurricane Andrew indicated that approximately 90% of severely damaged residences were in Wind Exposure B (suburban terrain) (NAHB 1993).

Records of insurance claims show that once the first roof sheathing panel was removed, the property damage losses are on the order of 80% of total insured properties (Sparks et al. 1994). Accordingly, the limit state for roof panel uplift is defined as the first failure (removal) of a panel. Severe wind pressures on a roof occur in the regions of flow separation at the eave, ridge, and corners of the roof. Panels at the roof corners are subject to the highest suction pressures. Furthermore, during wind load tests for residential roofs it has been found (Mizzell and Schiff 1994; Rosowsky and Schiff 1996) that an "equivalent tributary area" for a fastener in a critical location of a roof panel was on the order of 1 to 2 ft<sup>2</sup> (0.093–0.19 m<sup>2</sup>). Once failure of this single fastener occurred, the load was distributed to the surrounding fasteners causing failure to propagate throughout the panel.

Table 1 summarizes the wind load statistics for an enclosed

**Table 3.** Panel Uplift Capacity Statistics

Nail type/spacing	Mean	Coefficient of variation	Cumulative distribution function	Source
6d nails at 6 in./12 in. (150/300 mm)	25 psf (1.2 kPa)	0.15	Normal	Rosowsky and Schiff (1996)
8d nails at 6 in./12 in. (150/300 mm)	60 psf (2.87 kPa)	0.15	Normal	

structure (in which the nominal internal coefficient,  $GC_{pi}$  is  $\pm 0.18$ ). The wind load statistics were obtained from a Delphi study, supplemented by experimental data (Ellingwood and Tekie 1999). The demand (interface) variable for fragility assessment is the 3-s gust wind velocity,  $V$ , at 10-m elevation in Exposure C. All other variables in Eqs. (4)–(6) are modeled as random, as described in the following paragraphs. Parameter  $K_d$  accounts in an approximate way for the noncoincidence of building orientation and unfavorable wind direction. More sophisticated models involving matches of  $GC_p$  and extreme winds determined from the wind rose at specific sites lead to the observation that for buildings where the orientation to strong wind is unknown, wind pressures typically are 75–95% of the worst-case values computed from *ASCE standard 7* (Rigato et al. 2001). This observation is consistent with the statistics for  $K_d$  presented in Table 1.

### Dead Load

The dead load is assumed to remain constant in time. Its mean value is based on the weight of the roof, while its coefficient of variation is assumed to be 0.1. The dead load can be modeled by a normal distribution (Ellingwood et al. 1982). The statistics presented in Table 2 are based on the weight of the roof.

### Resistance to Wind Uplift

Table 3 summarizes statistics on resistance to uplift of 4 ft  $\times$  8 ft (1.2 m  $\times$  2.4 m) roof panels with various nailing patterns, while Table 4 summarizes statistics on capacities of two common roof-to-wall connection details. These statistics are based on laboratory tests of actual structural components; DOL effects are negligible, as noted earlier. For these data, the nominal diameters for “6d” and “8d” nails are assumed to be 0.113 and 0.131 in. (2.9 and 3.3 mm), respectively. The notation 6”/12” means that nails are spaced at 6 in. (152 mm) at the edges of the panel and at 12 in. (305 mm) in the interior of the panel. The H2.5 clip is a standard detail; the statistics are representative of its strength when installed per manufacturer recommendations.

Fig. 1 illustrates roof panel fragilities for the different roof configurations and nailing details summarized above. The maxi-

**Table 4.** Roof-to-Wall Connection Capacity Statistics

Connection type	Mean	Coefficient of variation	Cumulative distribution function	Source
3-8d toe nails	410 lbs (1.83 kN)	0.34	Normal	Reed et al. (1996)
H2.5 clip	1,312 lbs (5.84 kN)	0.10	Normal	

imum observed 3-s wind speed during Hurricane Andrew was approximately 165 mph (74 m/s). It should be noted that these results are not keyed to any particular code or standard; the structural components and systems analyzed are typical of residential construction in hurricane-prone areas, but these details may (or may not) be code-compliant in specific jurisdictions. Fig. 1 indicates that the roofs with roof panels installed with 6-d nails are almost certain to suffer severe damage under Hurricane Andrew-like conditions, with almost 100% certainty of losing of at least one panel. The failure rates of roof panels installed with 8d nails on roofs without overhang under similar wind conditions are approximately 60%. Fig. 2 shows the roof truss-to-wall connection fragility for one-story residences without a roof overhang in exposures B and C. The benefit of the hurricane clip over toe-nailing across the range of hurricane wind speeds is readily apparent.

Fig. 3 compares fragilities for both roof sheathing uplift and failure of the roof-to-wall connection for a one-story house (without a roof overhang) located in exposure B. It might be noted that the fragility for the 8d nailed roof panel appears to match the fragility for the 3-8d toe-nailed roof-to-wall connection closely. These two fragilities illustrate the concept of *balanced risk*. That is, if it were desired that each of the two dominant failure modes considered here should have the same failure probability, this pairing of construction details should be used (e.g., “8d” nailed roof panels with 3-8d toe-nailed roof-to-wall connection). Alternatively, if it is desired to ensure that roof sheathing removal occurs before failure of the roof-to-wall connection, one might specify, e.g., panels attached with 6d nails with the clip connection. This concept of using fragilities to compare relative risk and to make design decisions to achieve performance objectives (for one or more failure modes) suggests many other possible applications in light frame construction. For example, design decisions could be made based on an evaluation of fragilities to ensure a *sequence* of failure modes with increasing (wind, seismic, flood, or other) demand.

Validation of the hurricane wind fragility analysis presents a challenge due to the complex nature of hurricanes hazards, the mix of building types in an area affected by a natural disaster, and the lack of statistics suitable for modeling system behavior of light-frame wood construction. In a specific community under study, there would be a wide variety of building configurations because of various roof heights, roof slopes, house sizes, shapes, structural systems, ages, and governing building codes and design practices.

Comparisons are made of the predicted results with failures observed in post-disaster damage surveys (e.g., NAHB 1993, 1999a,b). Based on the information in these surveys, we assume a residential building inventory with 50% one-story houses with roof overhangs and 50% without roof overhangs. Among these houses, 70% have roof panels with 6d nails and 30% with 8d nails. Because the building inventory data were not complete (NAHB 1993), for illustrative purposes it was assumed that 90% of the roof-to-wall connections utilized a clip and 10% used 3 at 8d toe-nails. The fragilities for roof panels and roof-to-wall connection types estimated for this assumed mix of construction are illustrated in Fig. 4. The survey indicated that  $69 \pm 5\%$  of one-story houses lost at least one roof panel during Hurricane Andrew. The fragility analysis predicts a roof panel failure rate of 92%; however it is important to note that this is based on the *highest observed* peak gust wind speed. This value is not presumed to be representative over the entire study region; nor would it be expected that all structures are situated such that this maximum wind speed would be experienced. The limit state for roof panel

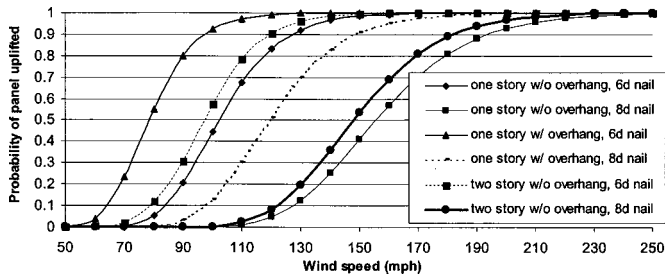


Fig. 1. Roof panel fragility of three typical house (exposure B)

uplift is modeled as the failure of the first panel based on research by Mizzell and Schiff (1994), which showed that once failure of a single fastener occurred, the load was distributed to the surrounding fasteners causing failure to propagate throughout the panel. Panels at the roof corner are subject to the highest uplift forces according to ASCE-7, where the local pressure coefficients,  $GC_p$ , are the highest of any point on the roof surface. Considering that the highest gust wind speed was assumed to apply to all houses in the postdisaster survey area and that the peak pressures acting on the roof occur over a very small area, this prediction can be viewed as a conservative upper bound on failure rate. Similarly, the predicted roof-to-wall failure rate was 11%, presuming that the resistance is similar to that provided by the H2.5 clip. If further detailed statistical data for the building inventory can be collected, the confidence in such estimates can be improved.

### Wind Fragility Sensitivity Analysis

In residential construction, building configurations and construction methods are highly variable. A parametric sensitivity analysis can identify the relative contribution of each uncertain variable to structural performance, providing insight on areas where to target further modeling and data collection. Such a parametric sensitivity study can deconstruct the fragilities of typical light-frame residential wood building structures into their dominant contributors, offering an efficient basis for improving building practice according to the relative contribution of each uncertain variable.

Table 1 shows the significance of exposure factor  $K_z$  (exposure B or exposure C). For the same building configuration, the mean wind load acting on the house increases 40% from exposure B (0.57) to exposure C (0.80), leading to an increase by a factor of 4 in the roof-to-wall clip connection failure rate (Fig. 2) at  $V = 165$  mph (74 m/s). Similarly, the exterior pressure coefficient  $GC_p$  is a dominant factor for roof panel uplift on houses with roofs with or without an overhang, because the roof overhang is located in a critical roof zone according to ASCE-7. In Fig. 1, the failure rate for roof panel with 8d nails of one-story gable roof

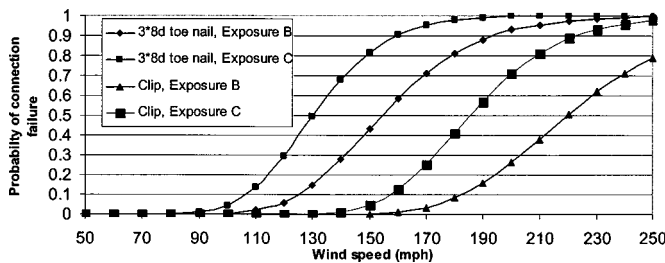


Fig. 2. Roof-to-wall connection fragility of one-story house without roof overhang

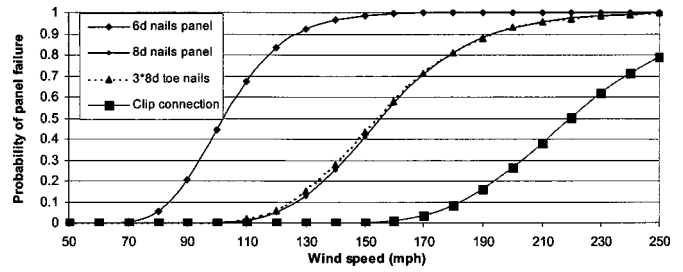


Fig. 3. Panel and roof-to-wall connection fragility (one story house without roof overhang, exposure B)

residential construction without and with roof overhang increases from 12 to 70% at  $V = 130$  mph (58 m/s). Conversely, Fig. 1 shows that the height of the house has little impact on fragility because exposure factor  $K_z$  is approximately the same for one-story and two-story houses.

Fastener selection and configuration is crucial if a house is to survive hurricane winds of the magnitude of Andrew, Opal, or Iniki. Nail size affects panel fragility significantly; 6d nails offer a mean resistance of only 25 psf (1.2 kPa) to uplift while 8d nails offer a mean resistance of 60 psf (2.9 kPa). This translates to a reduction by a factor of approximate 7 in failure rate for a one-story home without a roof overhang for wind speed in the 130 mph (58 m/s) range (see Fig. 1). For the roof-to-wall connection, the hurricane clip usually provides sufficient resistance to uplift while three 8d toenails do not. If the wind speed is 165 mph (74 m/s) in exposure B, 65% of roof truss-to-wall connections with three 8d nails in one-story houses without roof overhang will fail, but less than 5% will fail if a hurricane clip is provided (see Fig. 2). Finally, among all the factors, wind speed is the most significant because the pressure is proportional to the square of the wind speed. Accordingly, a network of accurate meteorological measurement systems is essential for regional damage and loss estimation.

### Seismic Fragility Analysis of Wood Panel Shear Walls

Performance-based design concepts for wood frame structures subjected to earthquake ground motion, such as those advanced by the CUREE-Caltech Wood Frame Project, are displacement-based and utilize the drift limits in FEMA 356 (2000). The results herein were obtained from a nonlinear dynamic time-history analysis of wood frame shear walls modeled as isolated subassemblies using *CASHEW*, a program developed as part of the CUREE-Caltech Wood Frame Project (Folz and Filiatrault 2001). *CASHEW* is a numerical model that predicts the load-

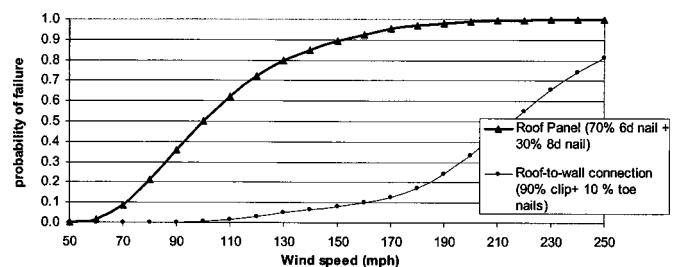


Fig. 4. Comparison of prediction with postdisaster (Andrew) survey

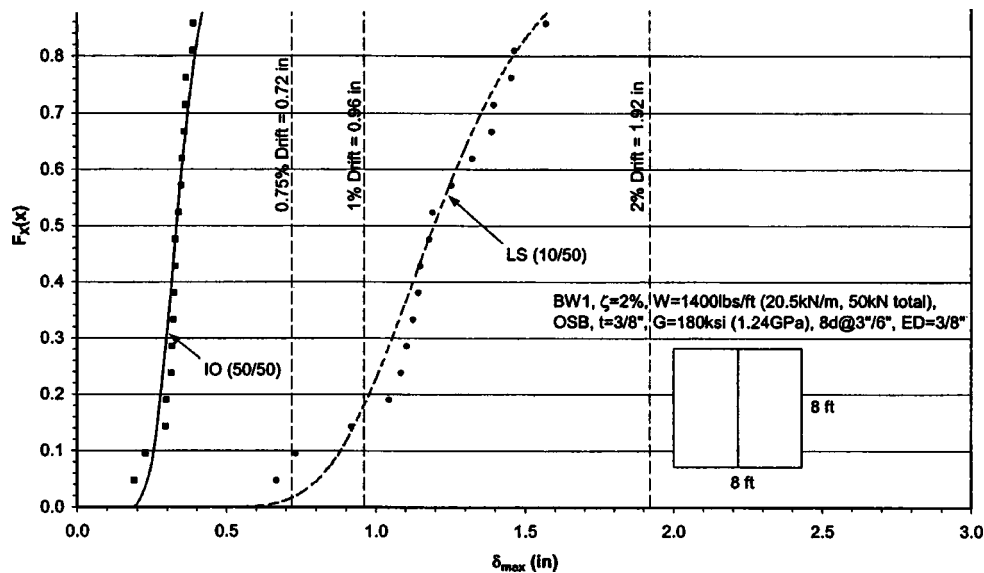


Fig. 5. Fitting a lognormal distribution to the sample CDF of peak displacements

displacement response of wood shear walls under quasi-static cyclic loading, taking into account the shear wall geometry, material properties, and the hysteretic behavior of the individual fasteners. This constitutive model of the wall defines parameters of an equivalent nonlinear SDOF model that can be used to predict the global cyclic response of a shear wall under arbitrary quasi-static cyclic loading or earthquake ground motions. The *CASHEW* program can only be used for bare walls (i.e., modeling the sheathing and fasteners only). For walls with nonstructural finish materials such as stucco or gypsum over the sheathing, parameters for the equivalent SDOF model were fit directly to hysteretic curves obtained from shear wall tests (Rosowsky 2002; Rosowsky and Kim 2002).

A suite of 20 ground motion records was used to characterize non-near fault ground motions in southern California. For the LS limit state, each record was scaled such that its mean 5% damped spectral value between periods of about 0.1 and 0.6 s matched the design spectral value of approximately 1.1g over the same period range recommended in the NEHRP Guidelines (FEMA 2000). This corresponds to the 10% in 50 years (10/50) hazard level. For the IO limit state, the records were scaled to the 50% in 50 years (50/50) hazard level using the same procedure. Seismic zone 4 and soil type D were assumed.

The greatest source of variability (or more specifically, contribution to the variability in peak response) arises from the ground motions themselves (i.e., the suite of 20 records characterizing the seismic environment in southern California). It was therefore decided to present the results obtained using each of the ground motions, scaled as appropriate for the limit state, in the form of a cumulative distribution function (CDF) of peak displacements. These distribution functions provide a convenient method for estimating probabilities of exceeding the stipulated FEMA 356 drift limits used to define the prescribed performance levels, e.g., 2% transient drift (LS) for the 10/50 hazard level, and 1% transient drift (IO) for the 50/50 hazard level. Once the peak displacement distributions were determined, they could be postprocessed into a form useful for design and/or assessment. Furthermore, by changing the spectral acceleration for the 20 records, a peak displacement CDF can be developed for each level of scaling. The probability of failure can be determined nonparametrically as the

relative frequency of the peak displacement exceeding the specified drift limit. This has the advantage of not requiring that a particular distribution function be fit to the peak displacements. For the example presented here, the records were scaled to five different hazard levels, ranging from 50% in 50 years, to 2% in 50 years. An illustration of this process is presented in Fig. 5.

The effect of different system parameters (material and structural) as well as construction quality levels on peak displacement were evaluated using this procedure by Rosowsky and Kim (2002). Selected results are included here for illustration. Fig. 6 shows the effect of fastener spacing on peak shearwall displacement for a staggered sheathing panel arrangement. In this example, the parameters are similar to those used to develop Fig. 5, except 5% damping and a higher shear modulus ( $G$ ) are assumed. As in the previous example (Fig. 5), the records are scaled for life safety (LS, 10/50 hazard level) and the corresponding FEMA 356 drift limit of 2% is shown for reference. The fastener is a 0.113 in. (2.9 mm) diameter pneumatically driven nail, and three different nailing patterns were considered. As expected, the change in perimeter nailing from 3 in. (75 mm) to 6 in. (150 mm) has the most significant effect on shear wall performance.

Fig. 7 shows the effect of missing fasteners in specific locations in the shear wall (with staggered sheathing panel arrangement as shown) on peak wall displacement. The parameters are the same as those in the previous figure, however, only one nailing pattern is considered, namely 3 in. (75 mm) along the perimeters and 6 in. (150 mm) in the field. The peak displacement distribution furthest to the left in this figure corresponds to the wall with no missing fasteners. As suggested in this figure, the walls having missing fasteners along the entire sole plate or at the midheight of the wall (at the horizontal blocking in the case of this wall layout) perform the worst. These types of figures can provide quantitative information about the effects of construction defects (or other tolerance information) on expected shearwall performance.

Fig. 8 shows the fragility curves for an 8 ft  $\times$  8 ft (2.4 m  $\times$  2.4 m) solid wall (no openings) with two full-size OSB sheathing panels [ $t=3/8$  in. (9.5 mm),  $G=200$  ksi (1.38 GPa)] oriented vertically. The walls were constructed using pneumatically driven 0.113 in. (2.9 mm) diameter nails spaced at 3 in./12 in. [3 in.

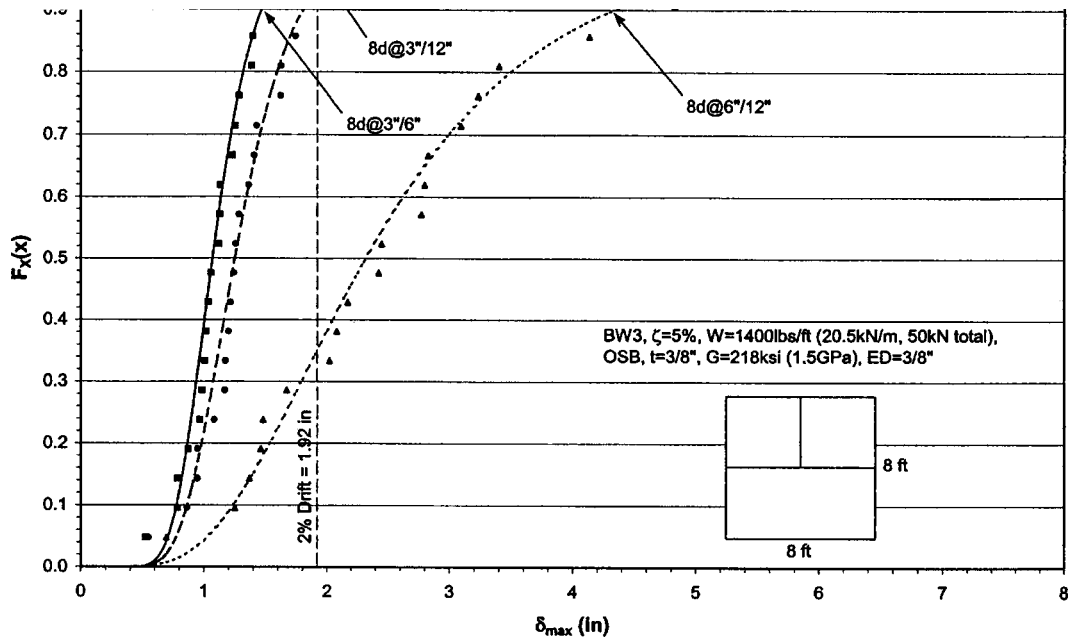


Fig. 6. Effect of fastener spacing on peak displacement

(75 mm) along the perimeters and 12 in. (300 mm) in the field]. The wall is assumed to be fully anchored. The effective seismic weight acting on the wall was determined based on the allowable shear values in the 1997 UBC. Drift limits of 1, 2, and 3% were considered. The seismic demand (interface) variable is the spectral acceleration,  $S_a$ . Fragility curves of this type can be used either as design aids or to assess risk consistency in current design provisions.

Using the same 8 ft  $\times$  8 ft (2.4 m  $\times$  2.4 m) shear wall with no openings, but considering only life safety (10% in 50 years hazard level, drift limit=2%), CASHEW was used to evaluate force-deformation relations for walls constructed using different

nailing schedules (2 in./12 in., 3 in./12 in., 4 in./12 in., and 6 in./12 in.) and assuming different  $R$  factors. These walls were analyzed using the suite of 20 records (scaled as appropriate), assuming that all walls had the maximum seismic weight permitted by the UBC. The UBC allows an  $R$  factor of 5.5 for wood shear walls; however, lower values also were considered. The UBC walls provided relatively consistent levels of safety (Kim 2003), as evidenced by the fact that the resulting fragility curves were quite close for all nailing schedules. That is, the allowable seismic weights provided in the UBC for the different nailing schedules resulted in comparable levels of performance. This permits the results for the different nailing schedules to be combined

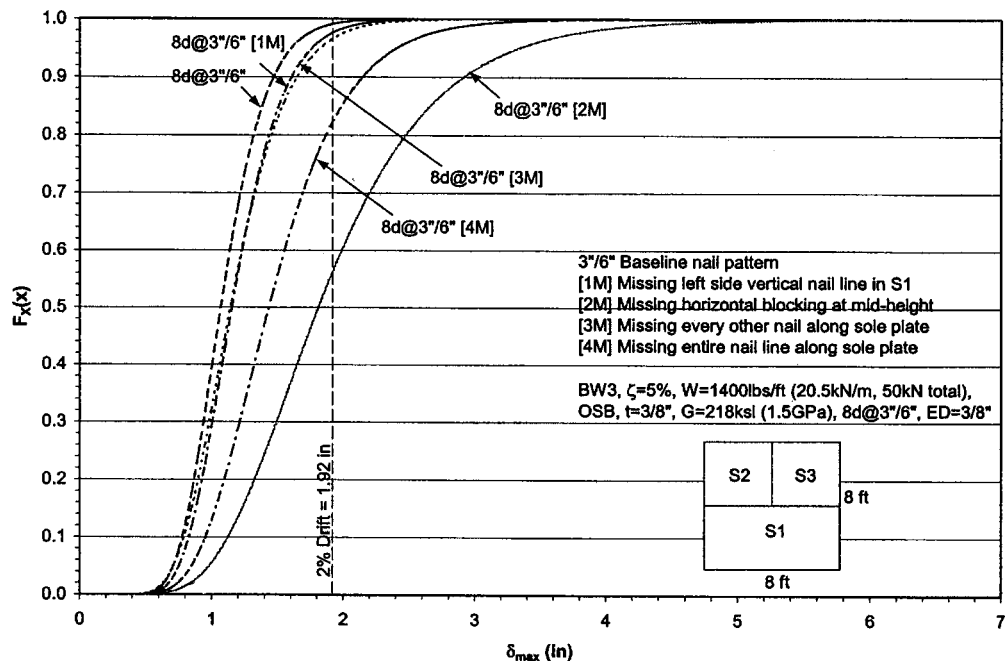
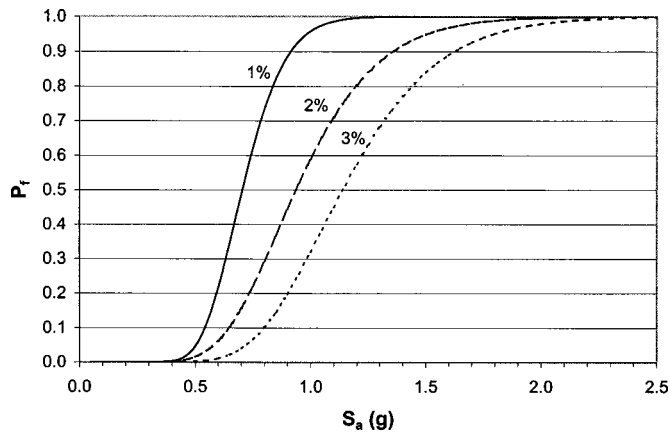


Fig. 7. Effect of missing fasteners on peak displacement





**Fig. 8.** Fragility curves for 8 ft  $\times$  8 ft shear wall designed using 1997 UBC (OSB sheathing, 0.113 in. diameter nail spaced at 3 in./12 in.)

to construct a single fragility curve for a given  $R$  factor. Fig. 9 shows the resulting fragility curves for the 8 ft  $\times$  8 ft (2.4 m  $\times$  2.4 m) shear wall considering life safety, for  $R$  factors ranging from 2.5 to 5.5.

### Perspectives on Risk and the Use of Fragility Models in Building Code Improvement

With the move toward performance-based engineering, it should become feasible to achieve residential building performance that is consistent with social needs. To do this effectively, the relative risks associated with performance under a spectrum of natural hazards must be understood. In some cases, mitigating one risk may reduce vulnerability to another, while in other cases vulnerability to other hazards might be increased. Standards and construction practice should aim at optimizing overall costs and risks.

In design for wind (and other nonseismic hazards), the product of the nominal load and load factor [i.e.,  $1.6W_n$  in Eqs. (4) and (6) of ASCE Standard 7-02] determines that level of wind hazard for design. In earthquake-resistant design, it has been customary to stipulate the design-basis earthquake directly [i.e.,  $1.0E_n$  in Eqs. (5) and (7) of ASCE 7-02]. In either case, these events correspond to an event with *approximately* a 10% probability of being ex-

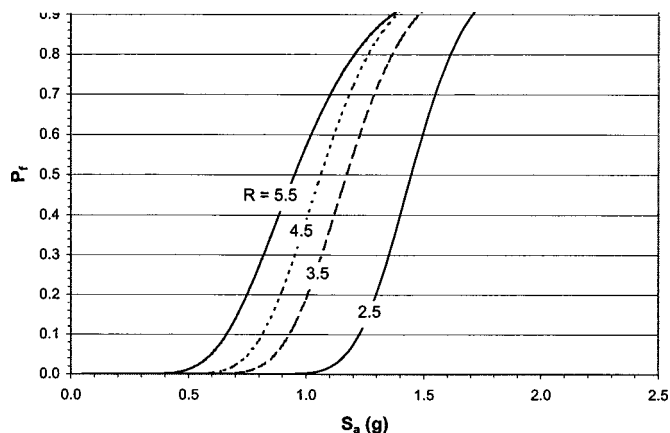


**Fig. 9.** Fragility curves for life safety (2% peak drift) for 8 ft  $\times$  8 ft shear wall designed using 1997 UBC and various  $R$  factors (OSB sheathing, 0.113 in. diameter nail)

ceeded in 50 years (a so-called 10% /50-year event, having a mean return period of approximately 500 years). This life safety performance objective, by and large, has been achieved for either natural hazard. On the other hand, code treatment of serviceability or loss of building function under lesser events has been uneven and, in some instances, nonexistent. Many clients now appear unwilling to accept the large economic losses that this single-minded focus on life safety has brought. Those who view their investment from a long-term rather than short-term perspective may be willing to pay for the higher level of performance. More sophisticated clients also may ask for a statement of confidence in whether the design will meet the stipulated performance objectives. Many stakeholders in the building process have some qualitative understanding of risk, but are poorly informed about quantitative risk analysis. The fragility—the likelihood of failure under a given event—is more easily explained, particularly when the control variable (wind speed; earthquake magnitude) is a parameter popularized in the media. It is easier for a nonspecialist to understand a statement like, “The probability is 90% that the typical home can be re-occupied immediately following the occurrence of a Simpson-Saffir Category 4 hurricane” than it is to understand the statement, “The probability of building failure is less than  $10^{-5}$ /yr.” Such small probabilities are difficult to interpret, even for risk analysts (Ellingwood 2001).

A comparative assessment of risks due to wind, earthquake, and similar natural hazards, while desirable for public policy and disaster planning purposes, as well as insurance underwriting, is difficult to perform at the current state of the art. Life safety is unlikely to be endangered significantly by hurricanes because the National Weather Service and civil authorities provide advanced warning of such events. On the other hand, the economic impact of building evacuation as well as damage to building contents is enormous. Severe earthquakes do not give advanced warning, making the life safety objective paramount. In either event, the disruptions and downtime in the local business community, as well as the need for certain essential facilities to maintain their integrity for postdisaster recovery, should factor into this comparative risk assessment.

The design-basis wind speed stipulated for Miami in ASCE 7-02 is a 3-s gust wind speed of 145 mph (65 m/s). Hurricane Andrew, with a maximum estimated wind speed of 165 mph (74 m/s) (Vickery et al. 1998), is believed to have been a 200- to 300-year event. Figs. 1 and 2 show that certain common construction practices (6d nailing of roof sheathing, toe-nailing roof trusses to walls) leads to an unacceptable rate of damage to roofs under such conditions. These estimates are consistent, in a qualitative sense, with postdisaster damage surveys conducted following Hurricane Andrew, and suggest improvements to building practices that would only minimally impact the cost of residential construction. Similarly (see Fig. 8), a light-frame wood shear wall building subjected to a 10% /50 (500-year) earthquake in Los Angeles County with a spectral acceleration  $S_a=0.7g$  at a period of 0.3 s has nearly a 50% probability of suffering sufficient damage to require minor structural repairs prior to normal occupancy but less than 5% probability of being damaged to the extent that the building occupants are endangered by structural damage or falling debris. Such probabilities for the inventory of residential buildings, properly interpreted, provide a starting point for code improvement.

## Conclusions

The fragility methodology summarized herein has the potential for providing effective strategies for improving structural safety and performance and for mitigating social and economic losses from competing natural hazards. Initial applications appear promising, but the methodology must be validated as a tool in projecting losses from postulated natural hazards before being applied for building code improvements (e.g., ASCE Standard 7) or to loss assessment and insurance underwriting. Further comparisons should be made of the predicted results with failures observed in postdisaster damage surveys. Following such validations, implementation of such a methodology would lead to more predictable building performance and facilitate the introduction of PBE, thus improving the utilization of wood and wood-based composites, reducing the vulnerability of the building envelope, structural and foundation systems to natural hazards, and mitigating the consequent economic losses and social disruption brought on by the occurrence of hurricanes and earthquakes.

## Acknowledgments

The research described in this paper was supported, in part, by the National Science Foundation under Grant No. CMS-0049038. This support is gratefully acknowledged. However, the writers take sole responsibility for the views expressed in this paper, which may not represent the position of the NSF or their respective institutions.

## References

- American Society of Civil Engineers (ASCE). (2003). "Minimum design loads for buildings and other structures." *ASCE standard 7-02*, Reston, Va.
- Ellingwood, B. R. (1994). "Probability-based codified design: Past accomplishments and future challenges." *Struct. Safety*, 13(3), 159–176.
- Ellingwood, B. (1998). "Reliability-based performance concept for building construction." in *Struct. Eng. Worldwide (Proc. Struct. Eng. World Congress 1998)*, Elsevier, *Paper T178-4* (CD-ROM)
- Ellingwood, B. R. (2001). "Acceptable risk bases for design of structures." *Prog. Struct. Eng. Mater.*, 3, 170–179.
- Ellingwood, B., MacGregor, J. G., Galambos, T. V., and Cornell, C. A. (1982). "Probability-based load criteria—Load factors and load combinations." *J. Struct. Div. ASCE*, 108(5), 978–997.
- Ellingwood, B. R., and Rosowsky, D. V. (1991). "Duration of load effects in LRFD for wood construction." *J. Struct. Eng.*, 117(2), 584–599.
- Ellingwood, B. R., and Tekie, P. B. (1999). "Wind load statistics for probability-based structural design." *J. Struct. Eng.*, 125(4), 453–463.
- Federal Emergency Management Agency (FEMA). (1997). "NEHRP guidelines for the seismic rehabilitation of buildings." *Rep. FEM-273*, Washington, D.C.
- Federal Emergency Management Agency (FEMA). (2000). "Prestandard and commentary for the seismic rehabilitation of buildings." *FEMA 356*, Washington, D.C.
- Folz, B., and Filiatrault, A. (2001). "Cyclic analysis of wood shear walls." *J. Struct. Eng.*, 127(4), 433–441.
- Galambos, T. V., Ellingwood, B. R., MacGregor, J. G., and Cornell, C. A. (1982). "Probability-based load criteria: Assessment of current design practice." *J. Struct. Div. ASCE* 108(5), 959–977.
- Green, D. W., and Evans, J. W. (1987). *Mechanical properties of visually graded lumber*, Vols. 1–5, Forest Products Laboratory, USDA, Madison, Wis.
- Hamburger, R. O. (1996). "Implementing performance-based seismic design in structural engineering practice." *Proc., 11th World Conf. On Earthquake Engineering, Acapulco, Mexico, (Paper 2121)*, Elsevier, New York.
- Kim, J. H. (2003). "Performance-based seismic design of light-frame shearwalls." PhD thesis, Oregon State University, Corvallis, Ore.
- Manning, B. R., and Nichols, G. G. (1991). "Hugo lessons learned." *Proc., Hurricane Hugo One Year Later*, Benjamin A. Sill and Peter R. Sparks, eds., American Society of Civil Engineers, New York.
- Mizzell, D. P., and Schiff, S. D. (1994). "Wind resistance of sheathing for residential roofs." *Wind Load Test Facility Rep.*, Department of Civil Engineering, Clemson University, Clemson, S.C.
- NAHB. (1993). "Assessment of damage to single-family homes caused by Hurricanes Andrew and Iniki." *NAHB Research Center Rep.*, Upper Marlboro, Md.
- NAHB. (1999a). "An industry perspective on performance guidelines for structural safety and serviceability of one and two-family dwellings." *Research Center Rep.*, National Association of Home Builders, Upper Marlboro, Md.
- NAHB. (1999b). "Reliability of conventional residential construction: An assessment of roof component performance in hurricane Andrew and typical wind regions of the United States." *NAHB Research Center Rep.*, Upper Marlboro, Md.
- Reed, T. D., Rosowsky, D. V., and Schiff, S. D. (1996). "Roof rafter to top-plate connections in coastal residential construction." *Proc., International Wood Engineering Conf.*, New Orleans, La., 4, 458–465.
- Rigato, A., Chang, P., and Simiu, E. (2001). "Database-assisted design, standardization, and wind direction effects." *J. Struct. Eng.*, 127(8), 855–860.
- Rosowsky, D. V. (2002). "Reliability-based seismic design of wood shear walls." *J. Struct. Eng.*, 128(11), 1439–1453.
- Rosowsky, D. V., and Cheng, N. (1999a). "Reliability of light-frame roofs in high-wind regions, I: Wind loads." *J. Struct. Eng.*, 125(7), 725–733.
- Rosowsky, D. V., and Cheng, N. (1999b). "Reliability of light-frame roofs in high-wind regions, II: Reliability analysis." *J. Struct. Eng.*, 125(7), 734–739.
- Rosowsky, D. V., and Ellingwood, B. R. (1991). "System reliability and load-sharing effects in light-frame wood construction." *J. Struct. Eng.*, 117(4), 1096–1114.
- Rosowsky, D. V., and Ellingwood, B. R. (2002). "Performance-based engineering of wood frame housing: Fragility analysis methodology." *J. Struct. Eng.*, 128(1), 32–38.
- Rosowsky, D. V., and Kim, J. H. (2002). "Reliability studies." *CUREE Publication No. W-10*, CUREE-Caltech Woodframe Project, Richmond, Calif.
- Rosowsky, D. V., and Schiff, S. D. (1996). "Probabilistic modeling of roof sheathing uplift capacity." *Proc., Probabilistic Mechanics and Structural Specialty Conf.*, ASCE, Reston, Va., 334–337.
- Schierle, G. G., ed. (2001). "Woodframe project case studies." *CUREE Publication No. W-04*, CUREE-Caltech Woodframe Project, Consortium of Universities for Research in Earthquake Engineering, Richmond, Calif.
- Sparks, P. R., Schiff, S. D., and Reinhold, T. A. (1994). "Wind damage to envelopes of houses and consequent insurance losses." *J. Wind. Eng. Ind. Aerodyn.*, 53, 145–155.
- Unanwa, C. O., McDonald, J. R., Mehtab, K. C., and Smith, D. A. (2000). "The development of wind damage bands for buildings." *J. Wind. Eng. Ind. Aerodyn.*, 84, 119–149.
- Uniform Building Code (1997). *1997 Edition, International Conference of Building Officials*, Whittier, Calif.
- Vickery, P. J., Skerlj, P. F., Steckely, A. C., and Twisdale, L. A. (1998). *Simulation of hurricane risk in the United States using an empirical storm track modeling technique*, Applied Research Associates, Raleigh, N.C.